

High Resolution Ultrasound Imaging Using Frequency Domain Interferometry

— Suppression of Interference Using Adaptive Frequency Averaging —

Hirofumi Taki^{*a)} Member, Takuya Sakamoto^{*} Member
Makoto Yamakawa^{**} Member, Tsuyoshi Shiina^{***} Member
Toru Sato^{*} Member

(Manuscript received Feb. 29, 2012)

We have reported that frequency domain interferometry (FDI) imaging with the Capon method has the potential to acquire high range-resolution ultrasound images. The reported method employed uniform frequency averaging to suppress coherent interferences. In atmospheric radar imaging, adaptive averaging has proposed to perfectly suppress coherent interference. In the present study, we applied adaptive frequency averaging to the FDI imaging method and investigated its image quality in a simulation study, where the -6 dB bandwidth of the echo returned from an interface was 2.6 MHz. When two targets 0.1 mm apart from each other were located in a region of interest the FDI imaging method using uniform frequency averaging succeeded in estimating the interface ranges correctly; however, the estimated echo intensity was 6.3 dB lower than the true echo intensity. In contrast, the FDI imaging method using adaptive frequency averaging successfully estimated the interface ranges, and the estimated echo intensity was only 0.049 dB higher than the true one. These results indicate that the FDI imaging method using adaptive frequency averaging has excellent accuracy in the measurement of echo intensity, under the condition that the echo waveform returned from each target is the same as the waveform of the reference signal.

Keywords : ultrasound imaging, high-resolution, vascular ultrasound, frequency domain interferometry, frequency averaging

1. Introduction

Cardiovascular disease (CVD) is one of the main causes of mortality worldwide. Vascular ultrasound is a non-invasive imaging method that acquires images of arterial walls. The measurement of carotid artery thickness using ultrasonography (US) is considered to be useful in detecting early atherosclerosis⁽¹⁾⁻⁽³⁾. Therefore, improvement in the range resolution of vascular ultrasound is expected to enable the detection of CVD at an earlier stage.

We have reported that the frequency domain interferometry (FDI) imaging method with the Capon method has the potential to acquire high range-resolution vascular ultrasound images⁽⁴⁾⁻⁽⁶⁾. In US, the echoes returned from different targets are strongly correlated⁽⁷⁾⁽⁸⁾. Since the FDI method with a power minimizing method such as the Capon method does not work when the desired signal and interferences are correlated with each other⁽⁹⁾⁽¹⁰⁾, we employed uniform frequency averaging to suppress the correlation between the desired signal and interference. However, uniform frequency averaging cannot suppress the correlation perfectly, and this suppression depends on the bandwidth used for the uniform frequency averaging. When the suppression of the correlation is insufficient, the accuracy of the FDI imaging method in echo

intensity estimation deteriorates⁽¹¹⁾.

In atmospheric radar imaging, adaptive averaging has been proposed to more effectively suppress the correlation between the desired signal and interference⁽¹²⁾⁽¹³⁾. Adaptive averaging selects the optimum weights adaptively to perfectly suppress the correlation. In the present study, we applied adaptive frequency averaging to the FDI method with the Capon method, and evaluated the effect of adaptive frequency averaging on ultrasound imaging.

2. Materials and Methods

We applied the proposed method to each received signal in a scan line separately. The proposed method is based on the FDI imaging method with the Capon method using the whitening technique. We briefly describe the FDI imaging method with the Capon method, and subsequently explain the frequency averaging techniques.

2.1 FDI Imaging Method with the Capon Method

The FDI imaging method with the Capon method assumes that the frequency components of a signal returned from a target have the same intensity. Since US utilizes broadband signals, we should employ the whitening technique to correct the intensity of all frequency components uniformly⁽⁶⁾. The received RF signal in the frequency domain after whitening is expressed as follows:

$$\mathbf{X}_H = [X_{H1} \ X_{H2} \ \dots \ X_{HN}]^T, \dots\dots\dots (1)$$

$$X_{Hi} = X_{pi} X_{ri}^* / (|X_{ri}|^2 + \eta), \dots\dots\dots (2)$$

where η is a constant term for stabilization, N is the number of frequency component samples used for imaging, $[\]^T$ denotes the

a) Correspondence to: Hirofumi Taki. E-mail: hirofumi.taki@mb6.seikyoku.ne.jp
* Graduate School of Informatics, Kyoto University
Yoshida-honmachi, Sakyo-ku, Kyoto 606-8501, Japan
** Advanced Biomedical Engineering Research Unit, Kyoto University
Yoshida-honmachi, Sakyo-ku, Kyoto 606-8501, Japan
*** Graduate School of Medicine, Kyoto University
Yoshida-honmachi, Sakyo-ku, Kyoto 606-8501, Japan

transpose, and X_{Hi} , X_{Pi} and X_{Ri} are the i -th frequency component of a received RF signal after whitening, the i -th frequency component of a received RF signal before whitening, and the i -th frequency component of a reference RF signal without whitening, respectively.

The estimated intensity of the FDI imaging method with the Capon method at the depth $r/2$ is given by:

$$P_{\text{Cap}}(r) = \frac{1}{\mathbf{C}^T \mathbf{R}^{-1} \mathbf{C}}, \quad (3)$$

$$\mathbf{R} = \mathbf{X}_H \mathbf{X}_H^T, \quad (4)$$

$$\mathbf{C} = [e^{jk_1 r} \quad e^{jk_2 r} \quad \dots \quad e^{jk_N r}]^T, \quad (5)$$

where k_i is the i -th wavenumber of the frequency components of the received RF signal, and $[\]^T$ denotes the conjugate transpose.

2.2 Uniform Frequency Averaging When a received signal consists of multiple echoes, the (i_1, i_2) element of a covariance matrix \mathbf{R} is given by:

$$\begin{aligned} R_{i_1, i_2} &= X_{Hi_1} X_{Hi_2}^* \\ &= \sum_l \alpha_l \exp(-jk_{i_1} r_l) \sum_l \alpha_l \exp(jk_{i_2} r_l) \\ &= \sum_l |\alpha_l|^2 \exp\{-j(k_{i_1} - k_{i_2})r_l\} + \sum_{l_1, l_2} \alpha_{l_1} \alpha_{l_2} (g_A + g_B), \end{aligned} \quad (6)$$

$$g_A = \exp\{-j(k_{i_1} - k_{i_2})r_{l_1} - jk_{i_1} \Delta r\}, \quad (7)$$

$$g_B = \exp\{-j(k_{i_1} - k_{i_2})r_{l_1} + jk_{i_2} \Delta r\}, \quad (8)$$

$$\Delta r = r_{l_2} - r_{l_1}, \quad (9)$$

where l , l_1 and l_2 ($l_1 < l_2$) are target numbers, α_l is the amplitude of the echo returned from the l -th target and $r_l/2$ is the target depth of the l -th target. We introduce the assumption that the amplitude of each frequency component of an echo after whitening is independent of its frequency. The second term of the last line of Eq. (6) is the cross-correlation term between different targets.

Since the FDI imaging method with the Capon method assumes that there is no correlation between the desired signal and the interference, the correlation term should be sufficiently suppressed. In atmospheric radar, the cross-correlation term is suppressed by the temporal averaging. However, in vascular ultrasound, targets are not stationary, resulting in difficulty in employing temporal averaging.

The first term of the last line of Eq. (6), the auto-correlation term, is constant when $i_1 - i_2$ is constant. Since the averaging of a covariance matrix along the diagonal direction suppresses the cross-correlation term, frequency averaging averages sub-matrices along the diagonal direction, as shown in Fig. 1.

$$\mathbf{R}_A = \sum_{m=1}^M v_m \mathbf{R}_{S_m}, \quad (10)$$

$$\text{subject to } \sum_{m=1}^M v_m = 1, \quad (11)$$

$$R_{S_m, i_1, i_2} = R_{(i_1+m-1), (i_2+m-1)}, \quad (12)$$

where \mathbf{R}_A is a covariance matrix after frequency averaging, v_m is a real number, M is the number of the sub-matrices used for frequency averaging, R_{i_1, i_2} and R_{S_m, i_1, i_2} are the (i_1, i_2) elements of

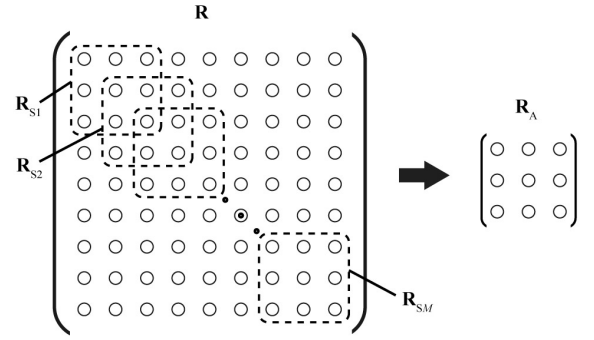


Fig. 1. The construction of the covariance matrix after frequency averaging, \mathbf{R}_A , from a covariance matrix \mathbf{R} .

a covariance matrix \mathbf{R} and a m -th sub-matrix \mathbf{R}_{S_m} , respectively.

Uniform frequency averaging employs a constant weight $v_m = 1/M$ ⁽⁶⁾. The covariance matrix after uniform frequency averaging \mathbf{R}_{UA} is given by:

$$R_{UA, i_1, i_2} = \sum_l |\alpha_l|^2 \exp\{-j(k_{i_1} - k_{i_2})r_l\} + \sum_{l_1, l_2} \alpha_{l_1} \alpha_{l_2} (\overline{g_A} + \overline{g_B}), \quad (13)$$

$$\begin{aligned} \overline{g_A} &= \frac{1}{M} \exp\{-j(k_{i_1} - k_{i_2})r_{l_1}\} \sum_{m=1}^M \exp(-jk_{i_1+m-1} \Delta r) \\ &\cong \exp\{-j(k_{i_1} - k_{i_2})r_{l_1}\} \frac{\sin(\pi F_A \Delta r / c)}{\pi F_A \Delta r / c} \\ &\quad \cdot \exp\{-2\pi j(F_{i_1} + F_A/2)\Delta r / c\}, \end{aligned} \quad (14)$$

$$\begin{aligned} \overline{g_B} &\cong \exp\{-j(k_{i_1} - k_{i_2})r_{l_1}\} \frac{\sin(\pi F_A \Delta r / c)}{\pi F_A \Delta r / c} \\ &\quad \cdot \exp\{2\pi j(F_{i_2} + F_A/2)\Delta r / c\}, \end{aligned} \quad (15)$$

where R_{UA, i_1, i_2} is the (i_1, i_2) element of the covariance matrix after frequency averaging \mathbf{R}_{UA} , F_A is the bandwidth used for frequency averaging, F_i is the i -th frequency and c is the sound velocity. These equations indicate that the cross-correlation term is suppressed in proportion to a sinc function of $\pi F_A \Delta r / c$. In the case of $F_A \Delta r / c < 0.5$ the FDI imaging method using uniform frequency averaging does not suppress the cross-correlation term sufficiently, causing deterioration in its performance. When the bandwidth for frequency averaging F_A is 2 MHz, the FDI imaging method using uniform frequency averaging drops into the severe situation under the condition of the target interval $\Delta r/2 < 0.2$ mm.

The estimated intensity of the FDI imaging method with the Capon method using uniform frequency averaging is given by:

$$P_{\text{CapUA}}(r) = \frac{1}{\mathbf{C}_A^T (\mathbf{R}_{UA} + \eta \mathbf{E})^{-1} \mathbf{C}_A}, \quad (16)$$

$$\mathbf{C}_A = [e^{jk_1 r} \quad e^{jk_2 r} \quad \dots \quad e^{jk_{N-M+1} r}]^T, \quad (17)$$

where $\eta \mathbf{E}$ is a diagonal loading matrix used to obtain the inverse matrix \mathbf{R}_{UA}^{-1} stably.

2.3 Adaptive Frequency Averaging Adaptive frequency averaging employs the optimum weight v_m to effectively suppress the cross-correlation term. When the cross-correlation term is perfectly suppressed, the (i_1, i_2) element of the covariance matrix after frequency averaging is given by:

$$R_{PA, i_1, i_2} = \sum_l |\alpha_l|^2 \exp\{-j(k_{i_1} - k_{i_2})r_l\}. \quad (18)$$

Therefore, the covariance matrix with no cross-correlation term becomes a Toeplitz matrix. Adaptive frequency averaging selects the weight v_m adaptively so as to approximate the covariance matrix to a Toeplitz matrix⁽¹²⁾.

The (i_1, i_2) element of the covariance matrix after frequency averaging is derived from Eqs. (10), (11) and (12).

$$R_{A_{i_1, i_2}} = \sum_{m=1}^M v_m R_{(i_1+m-1), (i_2+m-1)}, \quad \dots \quad (19)$$

The measure of deviation of the covariance matrix from a Toeplitz form is given by:

$$\varepsilon = \sum_{i'=0}^{L-2} \sum_{i=1}^{L-i'} |R_{A_{i, (i+i')}} - \overline{R_{A_{i'}}}|^2, \quad \dots \quad (20)$$

$$\begin{aligned} \overline{R_{A_{i'}}} &= \frac{1}{L-i'} \sum_{i=1}^{L-i'} R_{A_{i, (i+i')}} \\ &= \frac{1}{L-i'} \sum_{i=1}^{L-i'} \sum_{m=1}^M R_{(i+m-1), (i+i'+m-1)} = \sum_{m=1}^M v_m \overline{R_{S_{m, i'}}}, \quad \dots \quad (21) \end{aligned}$$

where $L = N - M + 1$ is the size of the covariance matrix after frequency averaging, and $\overline{R_{S_{m, i'}}$ is the average along the i' -th sub-diagonal of the m -th sub-matrix. Eq. (20) can be rewritten as follows:

$$\begin{aligned} \varepsilon &= \sum_{i'=0}^{L-2} \sum_{i=1}^{L-i'} \sum_{m=1}^M v_m \left\{ R_{(i+m-1), (i+i'+m-1)} - \overline{R_{S_{m, i'}}} \right\}^2 \\ &= \mathbf{V}^T \mathbf{R}_{\text{ce}} \mathbf{V}, \quad \dots \quad (22) \end{aligned}$$

where

$$\mathbf{V} = [v_1 \quad v_2 \quad \dots \quad v_M]^T, \quad \dots \quad (23)$$

$$\mathbf{R}_{\text{ce}} = \sum_{i'=0}^{L-2} \sum_{i=1}^{L-i'} \text{Re} \left\{ \mathbf{e}_{i, i'} \mathbf{e}_{i, i'}^T \right\}, \quad \dots \quad (24)$$

$$\mathbf{e}_{i, i'} = [e_{i, i', 1} \quad e_{i, i', 2} \quad \dots \quad e_{i, i', M}]^T, \quad \dots \quad (25)$$

$$e_{i, i', m} = R_{(i+m-1), (i+i'+m-1)} - \overline{R_{S_{m, i'}}}. \quad \dots \quad (26)$$

The minimization of ε under the constraint of Eq. (11) is expressed by

$$\min_{\mathbf{V}} \mathbf{V} \mathbf{R}_{\text{ce}} \mathbf{V}^T, \quad \dots \quad (27)$$

$$\text{subject to } \mathbf{V}^T \mathbf{I} = 1, \quad \dots \quad (28)$$

where

$$\mathbf{I} = [1 \quad 1 \quad \dots \quad 1]^T. \quad \dots \quad (29)$$

This problem can be solved by the application of Lagrange multiplier methods. The optimum vector \mathbf{V}_{opt} for the solution to (27) is given by:

$$\mathbf{V}_{\text{opt}} = \frac{(\mathbf{R}_{\text{ce}} + \eta' \mathbf{E})^{-1} \mathbf{I}}{\mathbf{I}^T (\mathbf{R}_{\text{ce}} + \eta' \mathbf{E})^{-1} \mathbf{I}}, \quad \dots \quad (30)$$

$$\text{subject to } \mathbf{V}^T \mathbf{I} = 1, \quad \dots \quad (31)$$

where $\eta' \mathbf{E}$ is a diagonal loading matrix to obtain the inverse matrix $\mathbf{R}_{\text{ce}}^{-1}$ stably. The employment of a large η' approximates \mathbf{V}_{opt} to a constant weight set employed in uniform frequency averaging.

The estimated intensity of the FDI imaging method with the Capon method using adaptive frequency averaging is given by:

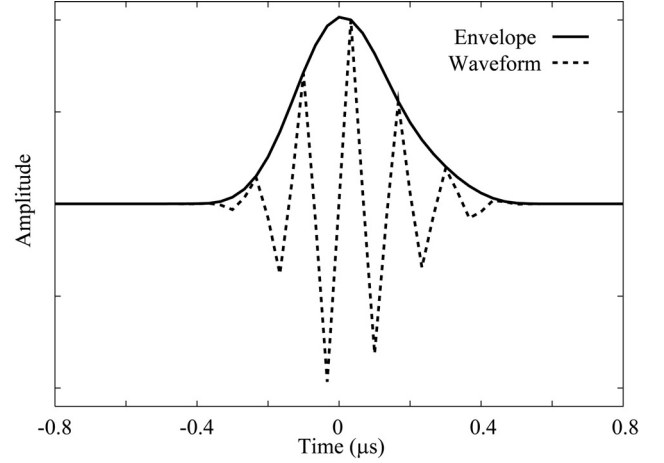


Fig. 2. Envelope and waveform of an echo returned from a horizontal interface between 20% gelatin and 4% agar.

$$P_{\text{CapAA}}(r) = \frac{1}{\mathbf{C}_A^T (\mathbf{R}_{AA} + \eta' \mathbf{E})^{-1} \mathbf{C}_A}, \quad \dots \quad (32)$$

$$\mathbf{R}_{AA} = \sum_{m=1}^M v_{\text{optm}} \mathbf{R}_{S_m}, \quad \dots \quad (33)$$

where v_{optm} is the m -th element of the optimum vector \mathbf{V}_{opt} .

2.4 Simulation Setup In the simulation study, we employed the echo returned from an interface between 20% gelatin and 4% agar acquired by a Hitachi EUB-8500 (Hitachi, Tokyo, Japan) US device with a 7.5 MHz linear array. The sampling frequency of the acquired RF data is 30 MHz. Fig. 2 shows the envelope and waveform of an echo returned from a horizontal interface. Since the -6 dB bandwidth of an echo returned from a horizontal interface is 2.6 MHz, the range resolution of a conventional imaging method using the intensity of the received signal is about 0.29 mm. In our study, we supposed the sound velocity c to be 1500 m/s.

We assume that a received signal is given by:

$$S(t) = \sum_l S'(g_l, t - r_l / c), \quad \dots \quad (34)$$

where $S'(g, t)$ is an echo returned from an interface whose slope angle is g degree, and $r_l/2$ is the depth of the l -th target. In the present study, we employed 6 echoes returned from interfaces with slope angles of 0, 2, 4, 6, 8 and 10 degrees. We used the echo from a horizontal interface as the reference signal.

The optimum stabilization term η at whitening is equal to the noise intensity of each frequency component. In our study, we employed the average intensity of the frequency components from 11 to 14 MHz as the value of η .

Since the loading of $\eta' \mathbf{E}$ is equivalent to the addition of white noise to the received signal, the employment of a small η' is desirable. We employed -40 dB of the average value of the diagonal terms of \mathbf{R}_A as the value of η' .

We used 54 frequency components from 5 to 9 MHz, where the frequency interval was 75 kHz. The bandwidth for frequency averaging was 2 MHz. We measured the depth from 10 to 20 mm, where the range interval was 0.01 mm.

3. Results

3.1 Targets of Horizontal Interfaces First, we investigated the performance of the FDI imaging method under

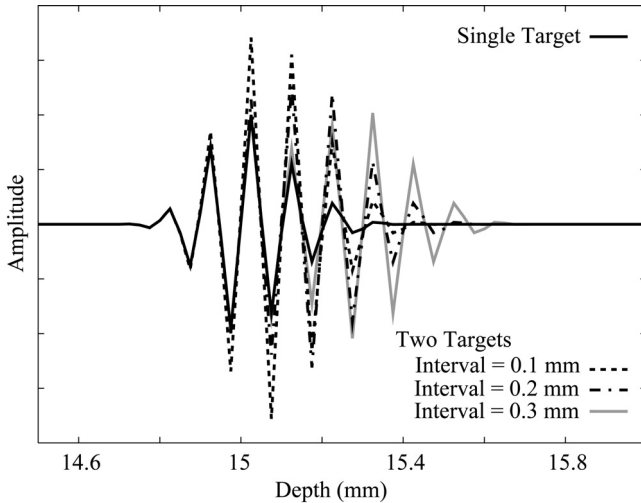


Fig. 3. Waveforms of the received signal returned from a single target and couples of targets, where target intervals of the target couples are 0.1, 0.2 and 0.3 mm and each target is a horizontal interface.

the condition that a couple of horizontal interfaces are located in a region of interest (ROI). In this case, the echo waveform returned from each interface is the same as the waveform of the reference signal. When the target interval is less than 0.3 mm, the conventional method using the intensity of the received signal could hardly depict the two targets separately, as shown in Fig. 3.

The FDI imaging method with the Capon method successfully estimated all the target depths correctly, as shown in Figs. 4 and 5. The FDI imaging method using uniform frequency averaging estimated the echo intensity returned from interfaces at 6.3, 1.6 and 0.19 dB lower than the true echo intensity when the target intervals were 0.1, 0.2 and 0.3 mm, respectively. The performance of the FDI imaging method using uniform frequency averaging in echo intensity estimation deteriorates severely when the target interval is 0.2 mm and less. Since we used a bandwidth of 2 MHz for uniform frequency averaging, this result is consistent with the consideration detailed at the end of section 2.2.

The FDI imaging method using adaptive frequency averaging estimated the echo intensity returned from interfaces at 0.049, 0.10 and 0.030 dB higher than the true echo intensity when the target intervals were 0.1, 0.2 and 0.3 mm, respectively. Here, we employed -40 dB of the average value of the diagonal terms of \mathbf{R}_{ee} as the value of η_V . This result suggests that adaptive frequency averaging is effective for the accurate estimation of echo intensity.

Fig. 6 shows the estimated intensity of the FDI imaging method using uniform frequency averaging and adaptive frequency averaging, where six horizontal interfaces are located in the ROI and the target interval is 0.3 mm. The performance of the FDI imaging method using adaptive frequency averaging in echo intensity estimation is superior to that using uniform frequency averaging. This result indicates that adaptive frequency averaging has an excellent accuracy in measuring echo intensity under the condition that the echo waveform returned from each target is the same as the waveform of the reference signal.

3.2 Targets of Sloped Interfaces We investigated the performance of the FDI imaging method under the condition that sloped interfaces are located in a ROI. For adaptive frequency

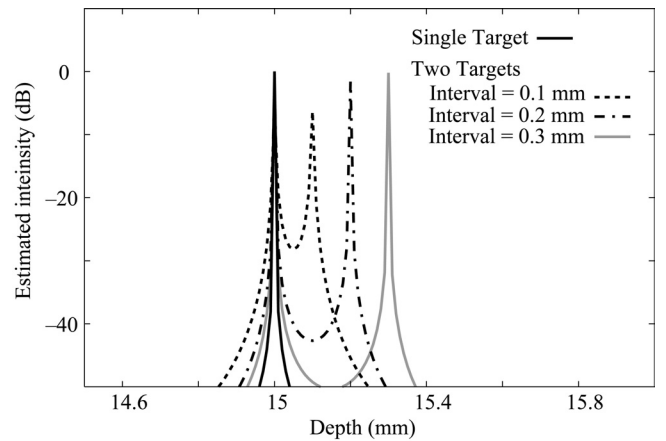


Fig. 4. Estimated intensity of the FDI imaging method using uniform frequency averaging. One and two horizontal interfaces are located in the ROI, and the target intervals are 0.1, 0.2 and 0.3 mm.

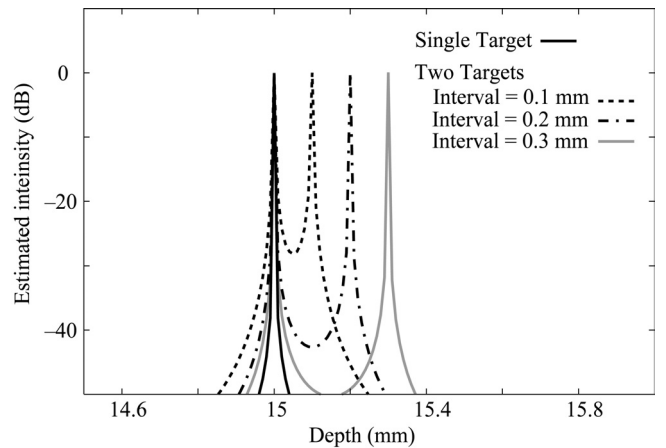


Fig. 5. Estimated intensity of the FDI imaging method using adaptive frequency averaging. One and two horizontal interfaces are located in the ROI, and the target intervals are 0.1, 0.2 and 0.3 mm.

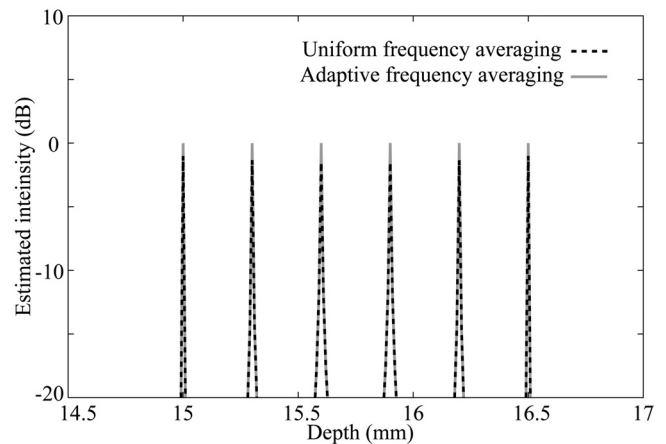


Fig. 6. Estimated intensity of the FDI imaging method using uniform frequency averaging and adaptive frequency averaging. Six horizontal interfaces are located in the ROI, and the target interval is 0.3 mm.

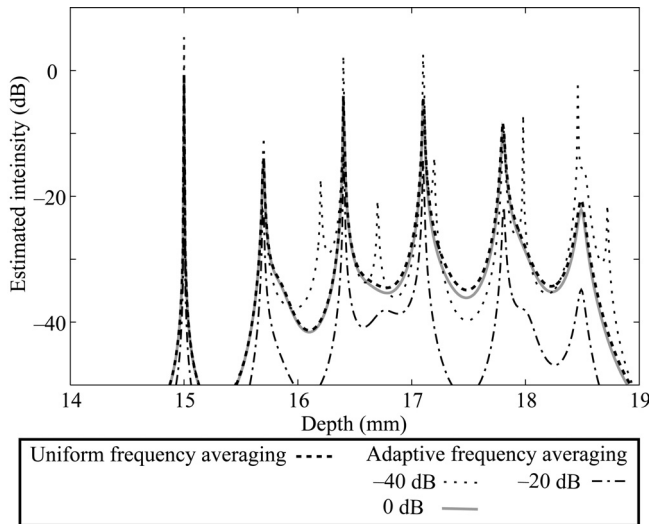


Fig. 7. Estimated intensity of the FDI imaging method using uniform frequency averaging and adaptive frequency averaging. Six interfaces are located at depths of 15, 15.7, 16.4, 17.1, 17.8 and 18.5 mm, where their slope angles are 0, 2, 4, 6, 8 and 10 degrees, respectively.

averaging we employed -40 , -20 and 0 dB of the average value of the diagonal terms of \mathbf{R}_{ee} as the value of η_V .

Fig. 7 shows that the estimated intensity of the FDI imaging method using uniform frequency averaging and adaptive frequency averaging. Six interfaces are located in the ROI, and their slope angles are 0, 2, 4, 6, 8 and 10 degrees. The employment of -40 dB diagonal loading for adaptive frequency averaging caused the appearance of false images. The employment of -20 dB diagonal loading for adaptive frequency averaging suppressed the appearance of false images; however, the performance of the imaging method is inferior to that using uniform frequency averaging in estimating the echo intensity returned from interfaces of large slope angles. The performance of the FDI imaging method employing 0 dB diagonal loading for adaptive frequency averaging is almost equivalent to that using uniform frequency averaging. This result indicates that adaptive frequency averaging is unsuitable under the condition where a received signal consists of echoes of various waveforms.

4. Discussion

The weighting vector \mathbf{V} should be composed of real numbers, as this constraint ensures that the auto-correlation terms, each of which is given by the first term of the last line of Eq. (6), are summed coherently and the information related to the target ranges is preserved. When the echo waveform returned from each target was the same as the waveform of the reference signal, elements of $\mathbf{e}_{l,l'}\mathbf{e}_{l,l'}^{T*}$ were real numbers, as shown in Fig. 8(a). Therefore, adaptive frequency averaging employing the optimum vector given by Eq. (30) successfully made the covariance matrix of a Toeplitz form. This means that adaptive frequency averaging sufficiently suppresses the cross-correlation term between different targets, resulting in accurate echo intensity estimation.

When the echo waveform returned from a target was different from the waveform of the reference signal, elements of $\mathbf{e}_{l,l'}\mathbf{e}_{l,l'}^{T*}$ had imaginary parts, as shown in Fig. 8(b). The appearance of imaginary parts is mainly caused at whitening. Since the echo

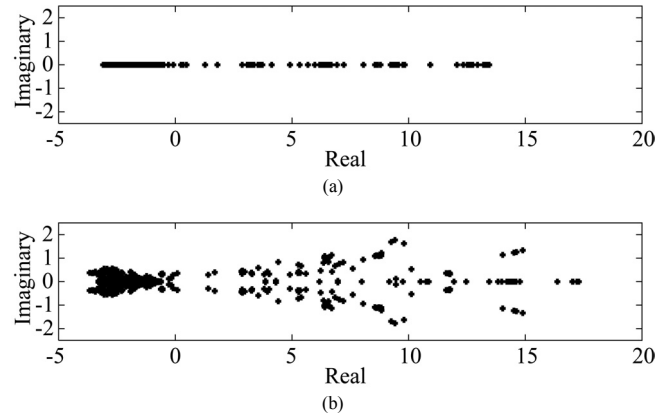


Fig. 8. Elements of $\mathbf{e}_{l,l'}\mathbf{e}_{l,l'}^{T*}$ at the calculation of the optimum vector \mathbf{V}_{opt} for adaptive frequency averaging. Six interfaces exist in a ROI, where (a) all interfaces are horizontal and (b) their slope angles are 0, 2, 4, 6, 8 and 10 degrees.

waveform returned from a sloped interface is different from the waveform of the reference signal, whitening fails in correcting the intensity of all frequency components uniformly. The appearance of imaginary parts at the elements of $\mathbf{e}_{l,l'}\mathbf{e}_{l,l'}^{T*}$ indicates that the covariance matrix does not become a Toeplitz matrix after adaptive frequency averaging. Therefore, the performance of the FDI imaging method using adaptive frequency averaging severely deteriorates under the condition where various sloped interfaces are located in a ROI.

This study demonstrates the effectiveness and limitation of adaptive frequency averaging. The FDI imaging method using adaptive frequency averaging does not work stably when the received signal consists of echoes of various waveforms; however, it delivers excellent performance under the condition that the echo waveform returned from each target is the same as the waveform of the reference signal. Therefore, we should locate a small ROI at an appropriate position to satisfy the constraint that the waveform of each echo included in the ROI is same as that of a reference signal. For example, a proper ROI may allow the imaging method for the estimation of carotid artery thickness.

5. Conclusion

In this study, we investigated the FDI imaging method with the Capon method using adaptive frequency averaging. When a received signal consists of echoes of various waveforms, the FDI imaging method using adaptive frequency averaging does not work stably. However, when two horizontal interfaces 0.1 mm apart are located in the ROI, the FDI imaging method using adaptive frequency averaging successfully estimates the interface ranges and the estimated echo intensity is 0.049 dB higher than the true one. Our study indicates that the FDI imaging method using adaptive frequency averaging has an excellent accuracy in measuring echo intensity as compared with the FDI imaging method using uniform frequency averaging, under the condition that the echo waveform returned from each target is the same as the waveform of the reference signal.

Acknowledgements

This work was partly supported by the Innovative Techno-Hub for Integrated Medical Bio-imaging Project of the Special Coordination Funds for Promoting Science and Technology from

the Ministry of Education, Culture, Sports, Science and Technology (MEXT), Japan.

References

- (1) J. J. P. Kastelein and E. D. Groot : "Ultrasound imaging techniques for the evaluation of cardiovascular therapies", *Eur. Heart J.*, Vol.29, pp.849-858 (2008)
- (2) M. L. Bots and D. E. Grobbee : "Intima media thickness as a surrogate marker for generalized atherosclerosis", *Cardiovasc. Drugs Ther.*, Vol.16, pp.341-351 (2002)
- (3) D. H. O'Leary and J. F. Polak : "Intima-media thickness: a tool for atherosclerosis imaging and event prediction", *Am. J. Cardiol.*, Vol.90, 18L-21L (2002)
- (4) H. Taki, T. Kimura, T. Sakamoto, and T. Sato : "High resolution medical acoustic vascular imaging using frequency domain interferometry", *Proc. IASTED Vis., Imag., Image Process.*, 652-038 (2009)
- (5) H. Taki, K. Taki, T. Sakamoto, M. Yamakawa, T. Shiina, and T. Sato : "High range resolution medical acoustic vascular imaging with frequency domain interferometry", in *Proc. IEEE EMBS*, pp.5298-5301 (2010)
- (6) H. Taki, K. Taki, T. Sakamoto, M. Yamakawa, T. Shiina, M. Kudo, and T. Sato : "High Range Resolution Ultrasonographic Vascular Imaging Using Frequency Domain Interferometry with the Capon Method", *IEEE Trans. Med. Imaging*, Vol.31, No.2, pp.417-429 (2012)
- (7) J. A. Mann and W. F. Walker : "A constrained adaptive beamformer for medical ultrasound: Initial results", in *Proc. IEEE Ultrason. Symp.*, pp.1807-1810 (2002)
- (8) J. F. Synnevag, A. Austeng, and S. Holm : "Minimumvariance adaptive beamforming applied to medical ultrasound imaging", in *Proc. IEEE Ultrason. Symp.*, pp.1199-1202 (2005)
- (9) B. Widrow, K. M. Duvall, R. P. Gooch, and W. C. Newman : "Signal cancellation phenomena in adaptive antennas: Causes and cures", *IEEE Trans. Antennas Propagat.*, Vol.30, No.3, pp.469-478 (1982)
- (10) W. F. Gabriel : "Spectral analysis and adaptive array super-resolution technique", *Proc. IEEE*, pp.654-666 (1980)
- (11) H. Taki, T. Sakamoto, M. Yamakawa, T. Shiina, and T. Sato : "Proper bandwidth for frequency averaging in medical ultrasound imaging using frequency domain interferometry", in *Proc. Symp. Ultrasonics Electronics*, pp.139-140 (2011)
- (12) K. Takao and N. Kikuma : "An adaptive array utilizing an adaptive spatial averaging technique for multipath environments", *IEEE Trans. Antennas Propagat.*, Vol.35, No.12, pp.1389-1396 (1987)
- (13) N. Kikuma, M. Yamada, and N. Inagaki : "Directionally constrained adaptive array using constraint modulus algorithm", In *Proc. ISAP*, pp.313-316 (1989)

Hirofumi Taki



(Member) received a M.D. degree from Kyoto University in 2000, a Ph.D. degree in informatics from Kyoto University in 2007, and is presently an assistant professor at Kyoto University. He has worked on development of the spatial resolution and calcification detection ability in Ultrasonography. IEEE, Japan Society of Ultrasonics in Medicine, Acoustic Society of Japan, The Institute of Electronics, Information and Communication Engineers, Japan Society for Medical and Biological Engineering member.

Takuya Sakamoto



(Member) received his B.E. degree from Kyoto University in 2000, and M.I. and Ph.D. degrees from the Graduate School of Informatics, Kyoto University in 2002 and 2005, respectively. He is an assistant professor in the Department of Communications and Computer Engineering, Graduate School of Informatics, Kyoto University. His current research interest is in ultra-wideband radar systems and ultrasonic signal processing. He is a member of the IEICE, the IEEJ and the IEEE.

Makoto Yamakawa



(Member) was born in Fukui, Japan, on May 8, 1975. He received a Ph.D. degree in engineering from University of Tsukuba in 2002, and is presently an associate professor at Kyoto University. He has worked on tissue characterization using ultrasound. Japan Society of Ultrasonics in Medicine, The Institute of Electronics, Information and Communication Engineers member.

Tsuyoshi Shiina



(Member) was graduated from the Electronic Engineering Department, the University of Tokyo, in 1982. He received the M.S. and Ph.D. degrees in electronic engineering in 1984 and 1987, respectively, from the University of Tokyo. He also received Dr. of Medical Science in 2006, from University of Tsukuba. He has been a Professor of Graduate School of Systems and Information Engineering, the University of Tsukuba since 2001. He is presently a Professor of Graduate School of Medicine, Kyoto University. His current research interests include visualization technique of structural and functional bio-information, for example, ultrasonic elasticity imaging and brain function imaging. He was awarded Prizes for Science and Technology about Real-Time Tissue Elasticity Imaging System by Minister of Education, Culture, Sports, Science and Technology, 2010. He is Councilor of the Japan Society of Medical Electronics and Biological Engineering. He is also Executive Trustee of the Japan Society of Ultrasonics in Medicine (JSUM).

Toru Sato



(Member) received his B.E., M.E., and Ph.D. degrees in electrical engineering from Kyoto University, Kyoto, Japan in 1976, 1978, and 1982, respectively. He is currently a Professor at Graduate School of Informatics, Kyoto University. His major research interests include system design and signal processing aspects of UWB radars and radar remote sensing of the atmosphere.